# Supplementary Information for

# Dissecting the Contributions to Non-photochemical Quenching in a Land Plant Under Fluctuating Light

Lam Lam[1,2]†, Rebecca Lee[3]†, Dhruv Patel-Tupper[2,4], Henry E. Lam[5], Tsung-Yen Lee[2,5], Alexa Ma[5], Sophia A. Ma[4], Hetty He[9], Krishna K. Niyogi[2,4,6,7]and Graham R. Fleming[1,2,5,8*]

[1]Graduate Group in Biophysics, University of California, Berkeley, CA 94720, USA.

[2]Molecular Biophysics and Integrated Bioimaging Division, Lawrence Berkeley National Laboratory, Berkeley, CA 94720, USA.

[3]Department of Chemistry, University of California, Los Angeles, CA 90095, USA.

[4]Department of Plant and Microbial Biology, University of California, Berkeley, CA 94720, USA.

[5]Department of Chemistry, University of California, Berkeley, CA 94720, USA.

[6]Howard Hughes Medical Institute, University of California, Berkeley, CA 94720, USA.

[7]Innovative Genomics Institute, University of California, Berkeley, CA 94720, USA.

[8]Kavli Energy Nanoscience Institute, Berkeley CA 94720, USA.

[9]Department of Molecular and Cell Biology, University of California, Berkeley, CA 94720, USA.

†These authors contributed equally.

*Corresponding authors. E-mail: grfleming@lbl.gov

# Supplementary Figures and Tables

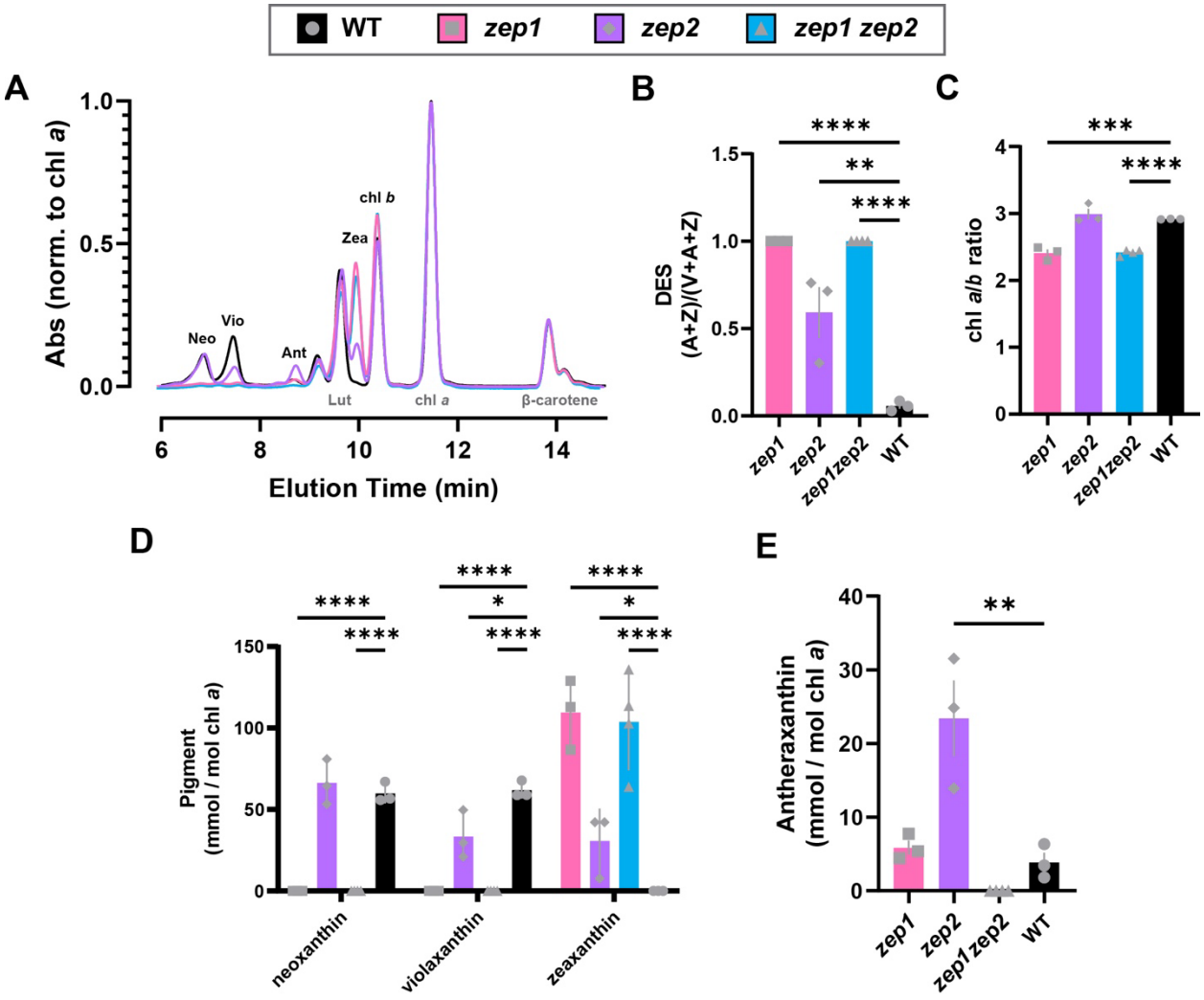


**Figure S1 Xanthophyll pigment profile of dark-acclimated *zep1*, *zep2*, and *zep1zep2* mutants.**

**A** Overlay of representative chromatograms normalized to chlorophyll *a*, resolving neoxanthin (Neo), violaxanthin (Vio), antheraxanthin (Ant), lutein (Lut), zeaxanthin (Zea), chlorophyll *b* (Chl *b*), chlorophyll *a* (Chl *a*), and β-carotene (β-Car) after 1 hour in darkness. **B** De-epoxidation state (DES). **C** Chl *a/b* ratio. **D, E** Individual xanthophyll pigment concentrations normalized to Chl *a*, with Ant plotted on a separate y-axis to increase contrast between genotypes. Data for dark-acclimated WT ($n = 3$, black, circle) is provided as a baseline against *zep1* ($n = 3$, pink, square), *zep2* ($n = 3$, purple, diamond), and *zep1zep2* ($n = 4$, blue, triangle). Data shown as mean ± 1 SEM. Pairwise significance was determined by ordinary one-way ANOVA (B, C, E; $\alpha = 0.05$) or two-way ANOVA (D, $\alpha = 0.05$) using Dunnett's test for multiple comparisons against WT, with significance denoted by asterisks (**$p \leq 0.01$, ***$p \leq 0.001$, **$p < 0.0001$).

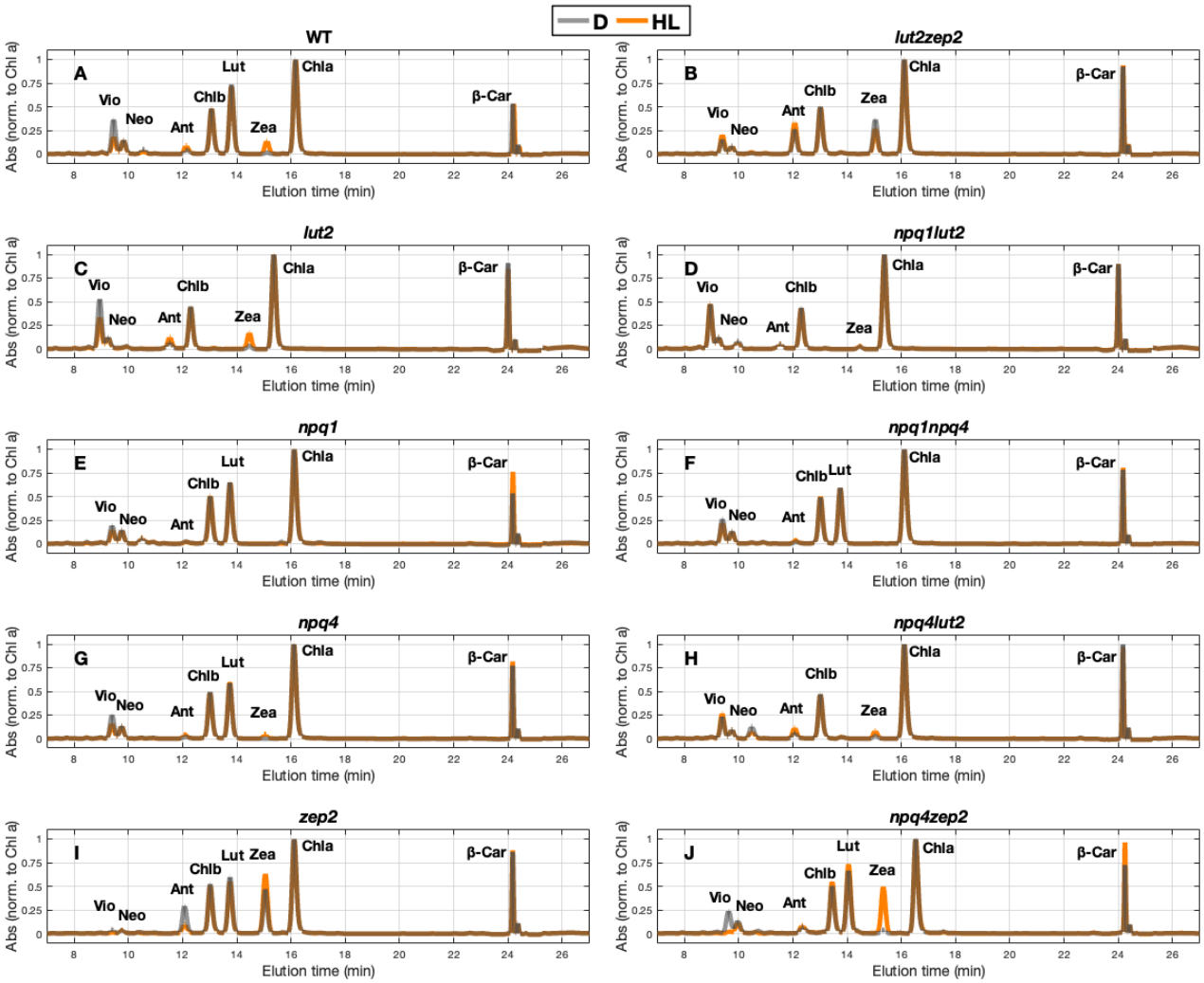


**Figure S2 Pigment profiles of *N. benthamiana* wild type (WT) and mutants.**

HPLC chromatograms showing pigment composition in whole-leaf extracts from: **A** WT, **B** *zep2 lut2*, **C** *lut2*, **D** *npq1lut2*, **E** *npq1*, **F** *npq1npq4*, **G** *npq4*, **H** *npq4lut2*, **I** *zep2*, **J** *npq4zep2*. Leaves were sampled after overnight dark acclimation (D, gray line) and following 15-min exposure to high light (HL, 1500 µmol photons $m^{-2}$ $s^{-1}$, orange line). Eight leaf disks (two per leaf) were pooled from four different leaves collected from three to four different plants. All chromatograms are normalized to Chl *a*. Major photosynthetic pigments are labeled at their respective elution times: Vio, Neo, Ant, Chl b, Lut, Zea, Chl *a*, β-Car.

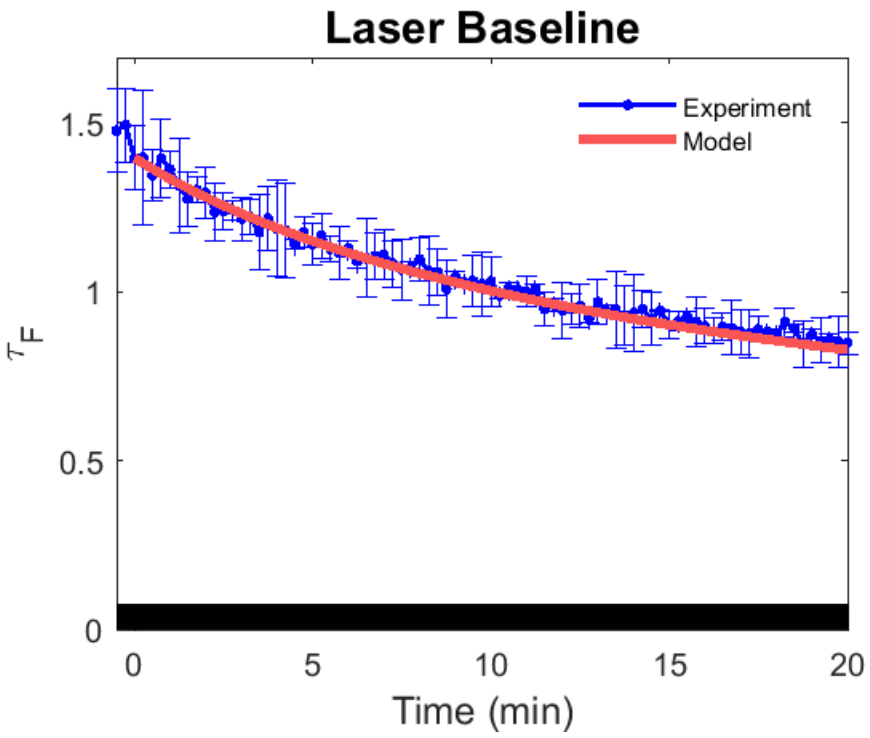


**Figure S3 Laser baseline chlorophyll fluorescence lifetime measurement on *npq1npq4* leaves (blue), and model fitting curve (red).** The model was fit to the laser baseline (no actinic light) alongside the *npq4npq1* lifetime measurements (n=3) in 20 min darkness (black bar). RMSD ($s^{-1}$) = 0.015. Error bars represent ± 2 SE from *n* biological replicates.

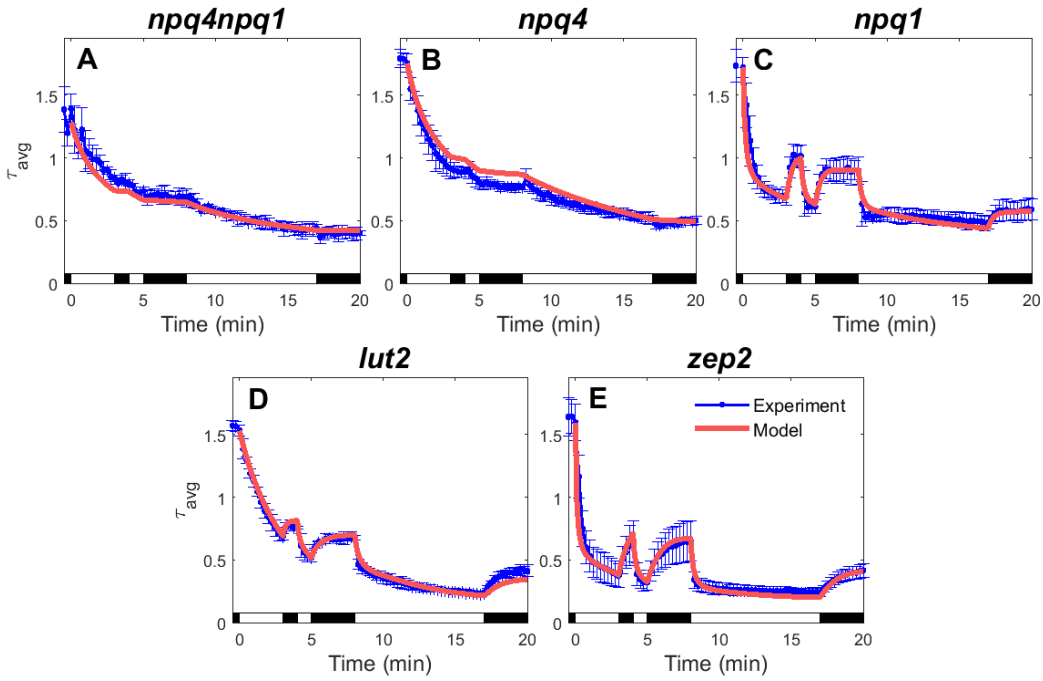


**Figure S4 Chlorophyll fluorescence lifetime measurement data (blue) and model fitting results (red) for single mutants under the 3HL–1D–1HL–3D–9HL–3D sequence. A** *npq4npq1* (n=3)*,* **B** *npq4 (n=3),* **C** *npq1* (n=6), **D** *lut2* (n=3), **E** *zep2* (n=9)**.** The 3HL–1D–1HL–3D–9HL–3D sequence was weighted equally with the 5HL-10D-5HL sequence in determination of best fit parameters. RMSD = **A** 0.049, **B** 0.105, **C** 0.115, **D** 0.264, **E** 0.404. White and black bars indicate high light (HL) and dark (D) phases of the actinic light sequence. Error bars represent ± 2 SE from *n* biological replicates.

**Table S1 Fitted parameters for NPQ kinetics for $\tau_F$ model under HL conditions.**

| Parameter | Value (HL) | Parameter | Value (HL) |
|---|---|---|---|
| $k_{va}^{L}$ | 2.17 | $k_{VDE}^{D}$ | 0.424 |
| $k_{va}^{D}$ | 0.016 | $k_{VDE}^{L}$ | 0.297 |
| $k_{az}^{L}$ | 0.425 | $k_{qZ}$ | 0.033 |
| $k_{av}$ | 1.30 | $k_{av,aba1}$ | 0.005 |
| $k_{za}$ | 0.033 | $k_{za,aba1}$ | 0.030 |
| $k_{PV,f}$ | 0.975 | $* k_{PV,f}$ | 1.25 |
| $k_{PV,b}$ | 10.49 | $* k_{PV,b}$ | 13.29 |
| $k_{PA,f}$ | 129.62 | $* k_{PA,f}$ | 36.0 |
| $k_{PA,b}$ | 253.25 | $* k_{PA,b}$ | 293.5 |
| $k_{PZ,f}$ | 294.72 | $* k_{PZ,f}$ | 74.5 |
| $k_{PZ,b}$ | 125.19 | $* k_{PZ,b}$ | 168.36 |
| $k_{QV,f}^{L}$ | 0.025 | $[V]_{0,npq1}$ | 49.66 |
| $k_{QV,b}$ | 0.0746 | $[V]_{0,lut2}$ | 75.0 |
| $k_{QA,f}^{L}$ | 0.402 | $[V]_{0,npq4}$ | 35.86 |
| $k_{QA,b}$ | 8.97 | $[V]_{0,aba1}$ | 10.84 |
| $k_{QZ,f}^{L}$ | 0.615 | $[V]_{0,\mathrm{WT}}$ | 35.86 |
| $k_{QZ,b}$ | 1.28 | $[P]_{tot}$ | 48.70 |
| $k_{QL,f}^{L}$ | 0.050 | $* [P]_{tot}$ | 49.74 |
| $k_{QL,b}$ | 3.54 | | |
| $k_{damage}^{L}$ | 0.0303 | | |
| $k_{damage}^{D}$ | 0.0035 | | |

Rate parameters are in units of $mmol \cdot mol\ Chl\ a^{-1} \cdot min^{-1}$. $k_{QX,f}$ is set to zero in dark conditions for all quenching species. * Denotes alternate *lut2* rates accounting for LHCII pigment composition changes. Lut concentrations were obtained from HPLC. The detailed description of the physical meanings of these parameters is provided in the Methods and Extended methods.

**Table S2 Quenching rate constants for Vio, Ant, Zea, and Lut in qE, as well as the rate constant for qZ and photoinhibition (qI).**

| Parameter | Value |
|---|---|
| $\kappa_{QV}$ | 0.045 |
| $\kappa_{QA}$ | 0.200 |
| $\kappa_{QZ}$ | 0.144 |
| $\kappa_{QL}$ | 0.238 |
| $\kappa_{qZ}$ | 0.033 |
| $\kappa_{qI}$ | 3.76 |
| † $\kappa_{qI}$ | 7.04 |

Quenching rates are a function of species concentration, expressed as $k_X = \kappa_X[X]$, where $[X]$ represents xanthophyll concentration (mmol/mol Chl *a*). † Denotes alternate qI quenching rate for double mutants.

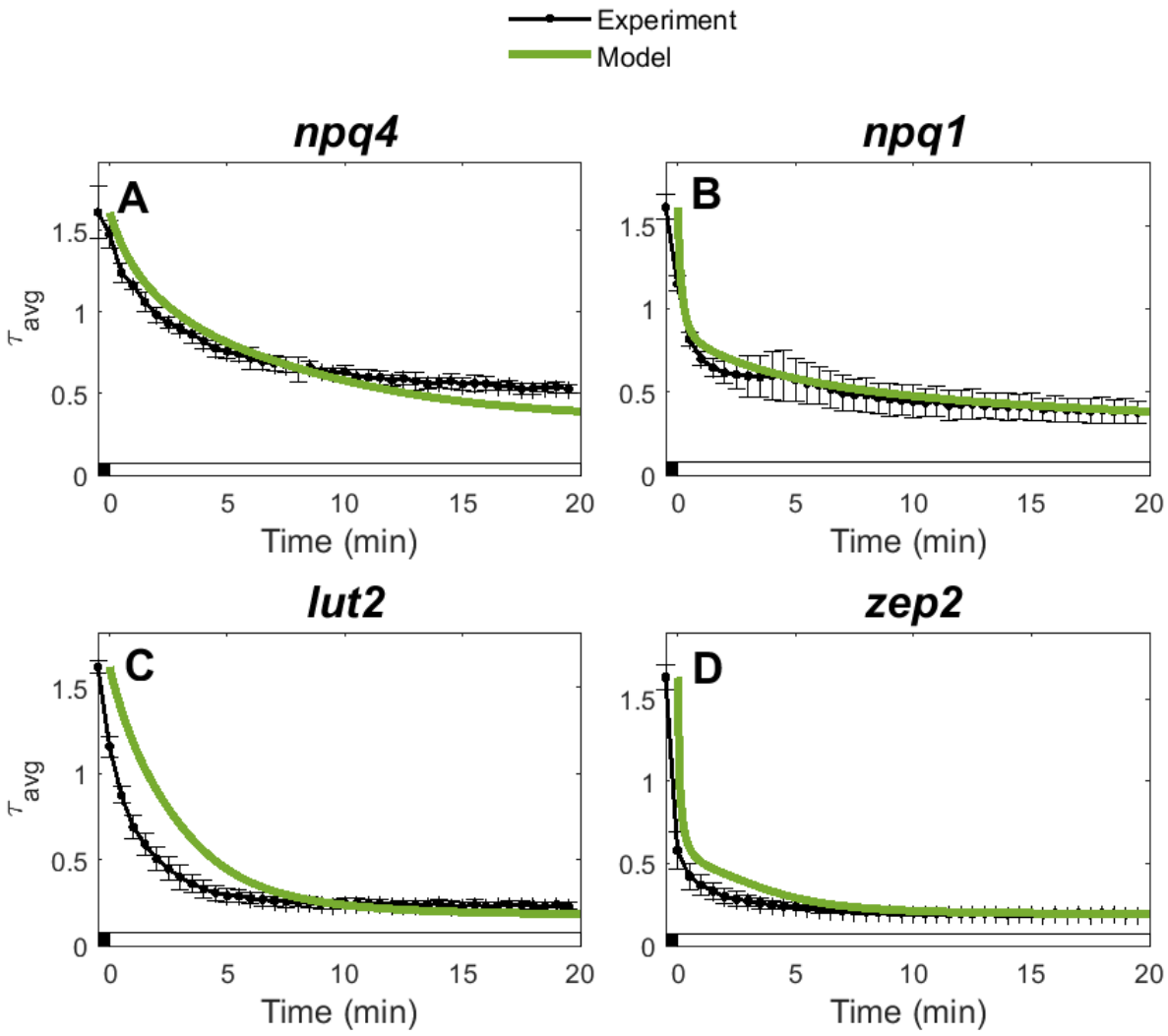


**Figure S5 Chlorophyll fluorescence lifetime measurement data (black) and model predictions (green) for single mutant sequences under the 20HL sequence. A** *npq4* (n=3), **B** *npq1* (n=4), **C** *lut2* (n=3), **D** *zep2* (n=4). Model predictions were calculated from parameters fitted in Figure 2 and Figure S4. RMSD values for the fits are ($s^{-1}$): **A** 0.330, **B** 0.094, **C** 0.754, **D** 0.433. A white and a black bar indicate high light (HL) and dark (D) phases of the actinic light sequence. Error bars represent ± 2 SE from *n* biological replicates.

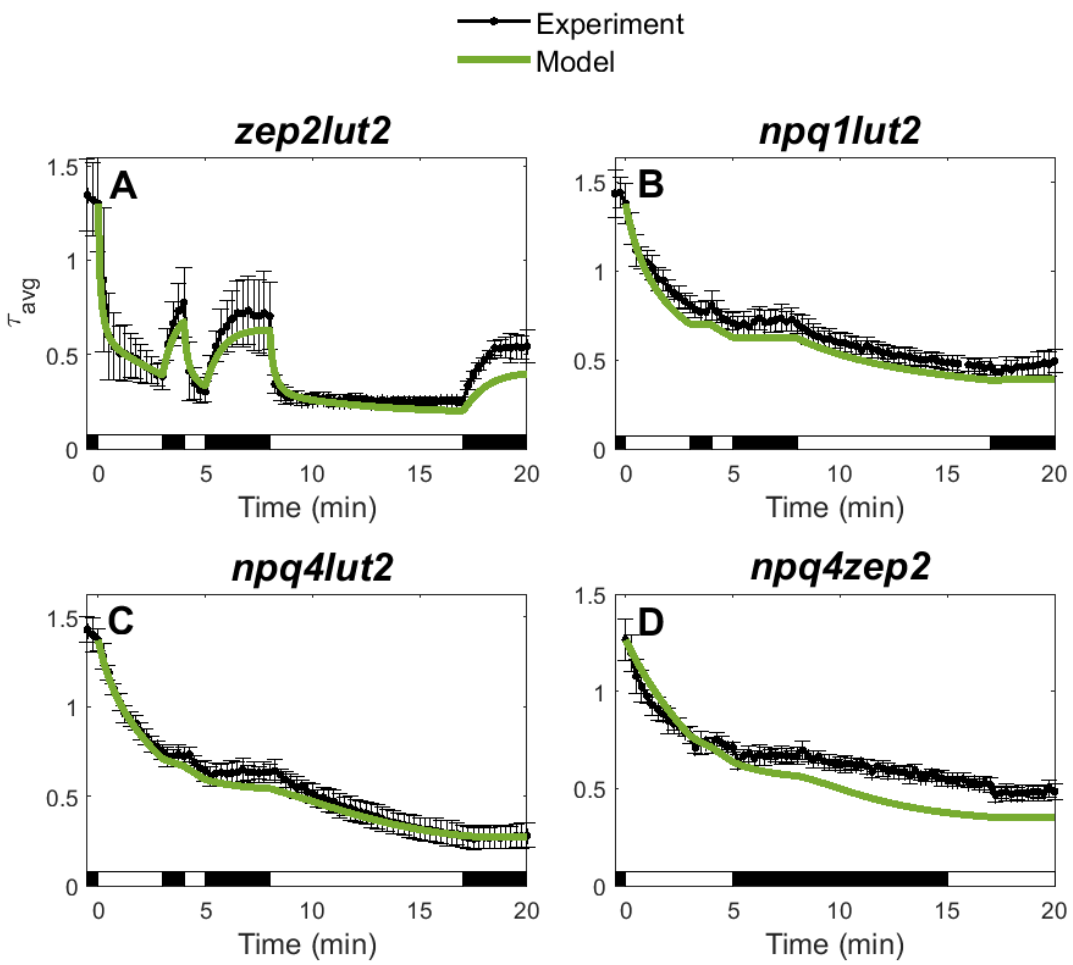


**Figure S6 Model predictions (green) and experimental validation (black) via chlorophyll fluorescence lifetime in double mutants under the 3HL-1D-1HL-3D-9HL-3D sequence. A** *zep2lut2* (*n*=3), **B** *npq1lut2* (*n*=4), **C** *npq4lut2* (*n*=4), **D** *npq4zep2* (*n*=4). Model predictions were calculated from parameters fitted in Figure 2 and Figure S4, with mutation-specific parameters combined to produce the modeled result. RMSD values for the fits are ($s^{-1}$) **A** 0.542, **B** 0.077, **C** 0.139 **D** 0.550. White and black bars indicate high light (HL) and dark (D) phases of the actinic light sequence. Error bars represent ± 2 SE from *n* biological replicates.

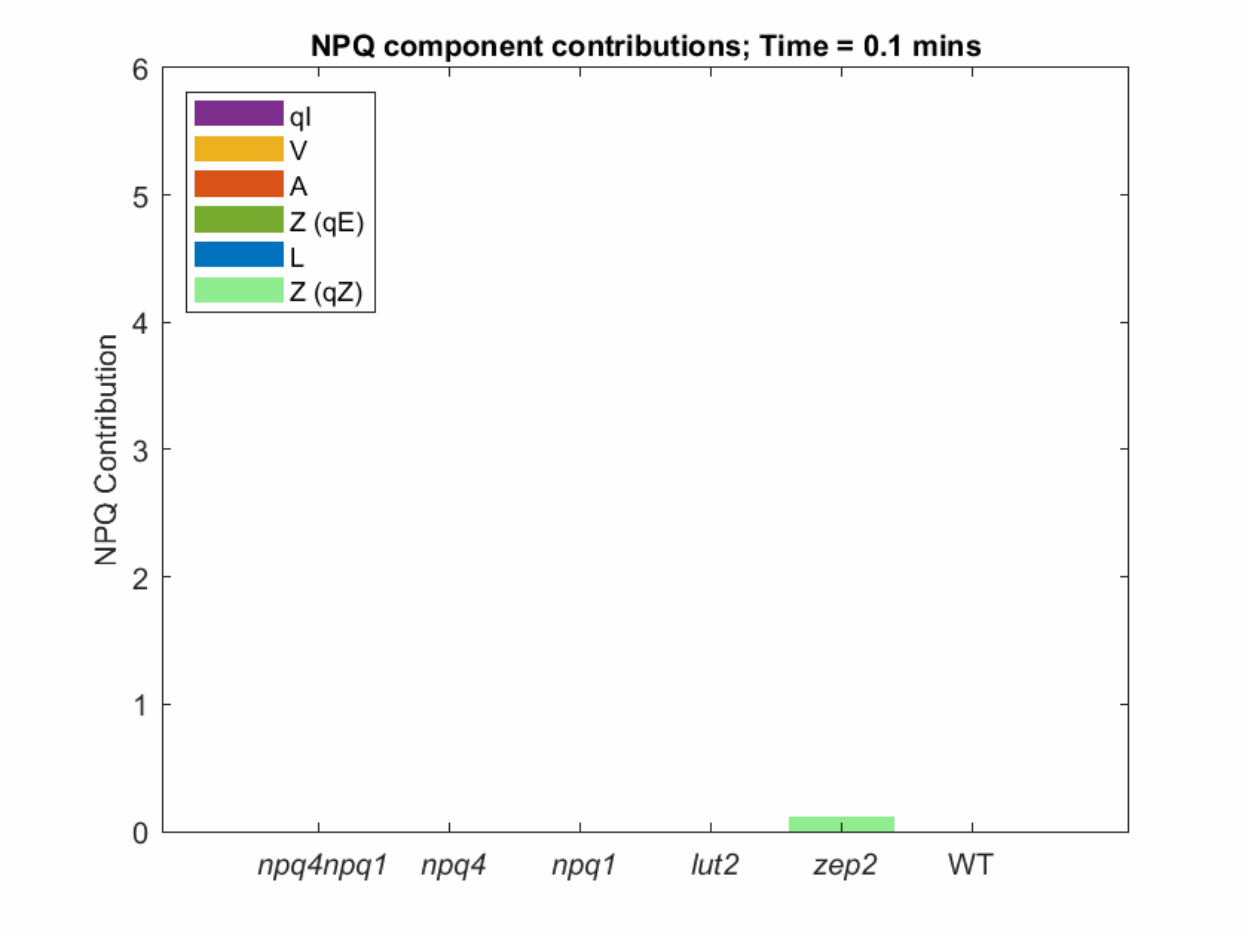


**Movie S1 NPQ contributions of qI, qE (V/A/Z/L), and qZ quenching components in *npq4npq1/npq4/npq1/lut2/zep2/*WT over time under continuous high light.** NPQ contributions were quantified component-wise by the linear relation $\kappa_{qX} \cdot QX(t)$ for each quenching xanthophyll $QX$, $\kappa_{qZ} \cdot Z(t)$ for qZ, and $\kappa_{qI} \cdot \alpha_{qI}(t)$ for qI. The sum of NPQ contributions may not be linearly proportional to overall Chl* quenching.

**(**The GIF file is provided separately as Supplementary Movie 1.)

**Table S3 *Arabidopsis thaliana ZEP* gene, the respective *N. benthamiana* orthologs, and gRNA target sites for CRISPR-Cas9 mutagenesis.**

| *A. thaliana* mutant | At Gene Locus | *N. benthamiana* Gene Name | Nb Genome Location | gRNA target site (from ATG) | Location | Spacer Sequences (5' -> 3') |
|---|---|---|---|---|---|---|
| *npq2 / aba1 / zep* | At5g67030 | ZEP1 | Niben101Scf16082g00007.1 | +296 : +316 | Exon 1 | GAAAAGGGGATTTGAGGTGT |
| | | | | +474 : +494 | Exon 1 | |
| | | ZEP2 | Niben101Scf01553g01001.1 | +296 : +316 | Exon 1 | GGTTTGGTTGATGGTGTTTC |
| | | | | +474 : +494 | Exon 1 | |

**Table S4 Primers for genomic DNA amplification of *N. benthamiana ZEP* genes.**

| Oligo ID | Oligo (5' -> 3') | Fragment Size | Tm |
|---|---|---|---|
| oNb11 ZEP_1.F | CCTCATTGGTTCAGCTTC | 806 bp | 58 |
| oNb12 ZEP_1.R | GACATGCAGTATTAAATGACACC | | |
| oNb13 ZEP_2.F | GGATTTCCCGACAGAGTTG | 530 bp | 58 |
| oNb14 ZEP_2.R | GCTTGTGTATGATTGTTACAGTGC | | |

**Table S5 Homozygous, Cas9-free *ZEP* knockout alleles of *N. benthamiana***

| $T_0$ Parent | Homozygous Progeny | *ZEP1* | *ZEP2* | Genotype | Mutant ID |
|---|---|---|---|---|---|
| ZEP_ko-4 | 38, 44, 58 | +1 bp | -6 bp | *zep1* | *zep1* |
| ZEP_ko-4 | 18, 39, 63 | -3 bp | -8 bp | *zep2* | *zep2* |
| ZEP_ko-4 | 46*, 68*, 72*, 88* | +1 bp | -8 bp | *zep1zep2* | *zep1zep2* |

* Indicates progeny that did not survive to seed set

**Table S6 Homozygous, Cas9-free higher-order mutants of *N. benthamiana* isolated by genetic crosses**

| Genetic Cross | Homozygous Progeny | ***PSBS1*** | ***PSBS2*** | ***VDE1*** | ***VDE2*** | Genotype | Mutant ID |
|---|---|---|---|---|---|---|---|
| *npq1* x *npq4* | #27-4-24 | -95 bp | +1bp | -5 bp | -60bp | *psbs1 psbs2 vde1 vde2* | *npq1npq4* |
| | | | | | | | |
| | | ***PSBS1*** | ***PSBS2*** | ***LUT2-1*** | ***LUT2-2*** | | |
| *npq4* x *lut2* | #25 | +1bp | +1bp | -3 bp | +1bp | *psbs1 psbs2 lut2-1 lut2-2* | *npq4lut2* |
| | | | | | | | |
| | | ***PSBS1*** | ***PSBS2*** | ***ZEP1*** | ***ZEP2*** | | |
| *npq4* x *zep2* | #72-15 | -8bp | -4 bp | -3bp/ WT | -8 bp | *psbs1 psbs2 zep2* | *npq4zep2* |
| | | | | | | | |
| | | ***VDE1*** | ***VDE2*** | ***LUT2-1*** | ***LUT2-2*** | | |
| *npq1* x *lut2* | #3-2, #3-20 | -11 bp | +1bp | +1bp | +1bp | *vde1 vde2 lut2-1 lut2-2* | *npq1lut2* |
| | | | | | | | |
| | | ***ZEP1*** | ***ZEP2*** | ***LUT2-1*** | ***LUT2-2*** | | |
| *zep2* x *lut2* | #2-7 | -3bp | -8bp | +1bp | +1bp | *zep2 lut2-1 lut2-2* | *zep2lut2* |

# Extended Methods

The kinetic scheme for our model of photoprotection in *N. benthamiana* is given in Methods. Within the model, each step is treated as an elementary reaction with rates as given, from which kinetic differential equations are constructed for each species. Explicitly, the kinetic differential equation system is as follows:

$$\frac{d}{dt}[V] = k_{av}[A] - k_{va}[VDE_a][V] - k_{PV,f}[V][P] + k_{PV,b}[PV] \tag{S.1}$$

$$\frac{d}{dt}[A] = k_{va}[VDE_a][V] + k_{za}[Z] - k_{az}[VDE_a][A] - k_{av}[A] - k_{PA,f}[A][P] + k_{PA,b}[PA] \tag{S.2}$$

$$\frac{d}{dt}[Z] = k_{az}[VDE_a][A] - k_{za}[Z] - k_{PZ,f}[Z][P] + k_{PZ,b}[PZ] \tag{S.3}$$

$$\frac{d}{dt}[PX] = k_{PX,f}[X][P] - k_{PX,b}[PX] - {k_{QX,f}}^{L/D}[PX] + k_{QX,b}[QX] \tag{S.4}$$

where $X = V, A, Z$

$$\frac{d}{dt}[PL] = {k_{QL,b}}[QL] - {k_{QL,f}}^{L/D}[PL] \tag{S.5}$$

$$\frac{d}{dt}[QX] = {k_{QV,f}}^{L/D}[PX] - k_{QV,b}[QX] \tag{S.6}$$

where $X = V, A, Z$

$$\frac{d}{dt}[\alpha_{qI}] = {k_{damage}}^{L/D}\tau_F(1 - \alpha_{qI}) \tag{S.7}$$

$$\frac{d}{dt}[\alpha_{VDE}] = k_{VDE}^{L/D}\left(\alpha_{vde,eq}^{L/D} - \alpha_{vde}\right) \tag{S.8}$$

Light/dark (L/D) dependent rate constants take different values depending on light conditions at time *t* during the sequence of light exposures. These values are fit independently,

with $k^{L/D} \equiv k^{L/D}(t) = k^{L}$ if HL at time *t*, or $k^{D}$ if D at time *t*. We set ${k_{QX,f}}^{D}$ to zero, assuming zero QX activation in dark.

The derivation and rationale for dynamical variables $\alpha_{VDE}(t)$ and $\alpha_{qI}(t)$ is given in Methods. We approximate $k_{va/az}(t) = k_{va/az,max}^{L/D} \cdot \alpha_{vde_a}(t)$ and directly fit the maximum rates $k_{va/az,max}^{L/D}$ in the model.

Model parameters are quantified using a least squares fit of experimental data to a calculated Chl *a* fluorescence lifetime. The time-dependent expression for $\tau_F$ is:

$$\tau_F(t) = \frac{1}{k_{r,nr} + \sum_X \kappa_X[QX] + \kappa_{qZ}[Z] + \kappa_{qI}\alpha_{qI}} \quad \text{(S.9)}$$

Derivation of this formula is given in Methods. This formulation allows for the direct quantification of quenching rates and per-molecule efficiencies of the individual quenchers while accounting for genotype-dependent variations in $\tau_{dark}\ (t = 0)$. In this model, $\kappa_{qX,}\ \kappa_{qZ,}\ \kappa_{qI}$ are additional fitting parameters representing the rate of Chl *a* exciton decay per molecule of quencher ($s^{-1}$(mmol/mol Chl *a*)$^{-1}$). $k_{r,nr}$ is calculated directly from $\tau_{dark}\ (t = 0)$ for each mutant dataset as $\frac{1}{\tau_F(0)} - \kappa_{qZ}[Z]_0$, assuming zero initial qE quenching, zero initial qI, and qZ calculated from initial zeaxanthin concentration. Thus, the model always requires an input estimate of $\tau_{dark}$. For genotypes with standard NPQ recovery capabilities, $[Z]_0 \approx 0$, so the expression simplifies to $\frac{1}{\tau_F(0)}$.

$\tau_F(t)$ is calculated directly from the solution set to the kinetic differential equation system produced by the model (using *ode23t* in MATLAB).